

Role of ERK1/2 in Platelet Lysate-Driven Endothelial Cell Repair

Elia Ranzato,^{1,2*} Francesca Boccafoschi,³ Laura Mazzucco,⁴ Mauro Patrone,¹ and Bruno Burlando¹

¹Department of Environment and Life Sciences, University of Piemonte Orientale “Amedeo Avogadro”, viale T. Michel 11, 15121 Alessandria, Italy

²Molecular Histology and Cell Growth Unit, San Raffaele Scientific Institute, via Olgettina 58, 20123 Milano, Italy

³Clinical and Experimental Medicine Department, University of Piemonte Orientale “Amedeo Avogadro”, via Solaroli 17, 28100 Novara, Italy

⁴Department of Haematology & Blood Transfusion Medicine, Azienda Ospedaliera Nazionale SS. Antonio e Biagio e C. Arrigo, via Venezia 16, 15121 Alessandria, Italy

ABSTRACT

Mechanisms of endothelial repair induced by a platelet lysate (PL) were studied on human (HuVEC, HMVEC-c) and non-human (PAOEC, bEnd5) endothelial cells. A first set of analyses on these cells showed that 20% (v/v) PL promotes scratch wound healing, with a maximum effect on HuVEC. Further analyses made on HuVEC showed that the ERK inhibitor PD98059 maximally inhibited the PL-induced endothelial repair, followed in order of importance by the calcium chelator BAPTA-AM, the PI3K inhibitor wortmannin and the p38 inhibitor SB203580. The PL exerted a chemotactic effect on HuVEC, which was abolished by all the above inhibitors, and induced a PD98059-sensitive increase of cell proliferation rate. Confocal calcium imaging of fluo-3-loaded HuVEC showed that PL was able to induce cytosolic free Ca²⁺ oscillations, visible also in Ca²⁺-free medium, suggesting an involvement of Ins3P-dependent Ca²⁺ release. Western blot analysis on scratch wounded HuVEC showed that PL induced no activation of p38, a transient activation of AKT, and a sustained activation of ERK1/2. The complex of data indicates that, although different signalling pathways are involved in PL-promoted endothelial repair, the process is chiefly under the control of ERK1/2. *J. Cell. Biochem.* 110: 783–793, 2010. © 2010 Wiley-Liss, Inc.

KEY WORDS: ENDOTHELIAL CELLS; CONFOCAL CALCIUM IMAGING; PI3K; SCRATCH WOUND ASSAY; CELL MIGRATION ASSAY

The vascular endothelium consists of a continuous monolayer of cells lining the luminal surface of the vascular system and providing a structural and metabolic barrier between blood and the underlying tissues. A host of agents have been reported to cause endothelial injury and dysfunction, including cytokines, hypoxia, shear stress, oxidised lipids, elevated blood pressure, hyperglycemia, nicotine, free radicals and viral and immune injury [Gotlieb, 1997]. These agents may cause endothelial damage, so that endothelial cells lose cell–cell and cell–substratum adhesion, resulting in enhanced permeability across the endothelium. Endothelial repair and regeneration mechanisms are considered to play an important

role in the protection of the vessel wall from various diseases, primarily atherosclerotic plaque formation [Ross, 1993].

A plethora of materials for wound dressing, skin substitutes and recombinant growth factors related to wound healing have been shown to mimic or enhance the healing process, and some of them have been introduced into the clinical setting with therapeutic efficacy [Ovington, 2007]. Platelets have attracted much interest in this field, since they are rich in wound-healing mediators. The secretory platelet α -granules contain growth factors playing important roles in tissue restoration, such as basic fibroblast growth factor (bFGF), vascular endothelial growth factor (VEGF),

Abbreviations used: Ins3P, inositol-3P; PL, platelet lysate.

Grant sponsor: Ricerca Sanitaria Finalizzata, Regione Piemonte, Italy, 2008; Grant sponsor: University of Piemonte Orientale “Amedeo Avogadro”.

*Correspondence to: Dr. Elia Ranzato, DiSAV, University of Piemonte Orientale “Amedeo Avogadro”, viale T. Michel 11, 15121 Alessandria, Italy. E-mail: ranzato@mfu.unipmn.it

Received 17 November 2009; Accepted 18 February 2010 • DOI 10.1002/jcb.22591 • © 2010 Wiley-Liss, Inc.

Published online 5 April 2010 in Wiley InterScience (www.interscience.wiley.com).

platelet-derived growth factor (PDGF) and transforming growth factor β (TGF- β) [Martin, 1997]. In addition, platelet derivatives have been shown to induce a functional angiogenic response in vitro [Giusti et al., 2009], although the cellular mechanisms involved in this platelet-induced angiogenic stage of tissue repair have not been clarified yet.

In the present study, we have explored the mechanisms of endothelial damage repair induced by a platelet lysate (PL) on different endothelial cell types, including human (HuVEC, HMVEC-c) and non-human mammalian (PAOEC, bEnd5) models. This platelet derivative, which is obtained from repeated freezing–thawing of platelet-enriched blood samples, has been shown to accelerate the in vitro wound healing of skin cells [Ranzato et al., 2008, 2009b] and mouse myoblasts [Ranzato et al., 2009a]. It has been also used as a dressing in clinical practice to improve wound healing [Mazzucco et al., 2004].

In our experiments, we used in vitro scratch wound and cell migration assays, coupled to light microscope image analysis, Western immunoblotting and confocal calcium imaging. Our data showed that PL accelerates wound closure in endothelial cell monolayers. A more in depth analysis carried out on HuVEC cells showed that the effect of PL occurs through the stimulation of cell proliferation and migration. The process is strictly ERK1/2-dependent, while intracellular Ca^{2+} , PI3K and p38 play less important roles.

MATERIALS AND METHODS

REAGENTS

SB203580, PD98059, wortmannin and BAPTA-AM were from Calbiochem (La Jolla, CA); fluo-3/AM was from Invitrogen (Carlsbad, CA); all other reagents were from Sigma (St. Louis, MO).

CELL LINE AND PLATELET LYSATE (PL) PREPARATION

Experiments were conducted on different types of endothelial cells. HuVEC were obtained from umbilical cord of donor patients after informed consent, according to the method of Jaffe et al. [1973] with minor modifications. Umbilical cord samples were incubated in 0.2% collagenase type I solution (Boehringer-Mannheim, Germany) for 20 min at 37°C to allow endothelial cell detachment from the vessel wall. Isolated cells were cultured in M199 medium supplemented with 10% foetal bovine serum, 50 $\mu\text{g}/\text{ml}$ endothelial cell growth supplement (ECGS), glutamine (2 mM), penicillin (100 U/ml) and streptomycin (100 mg/ml), and incubated at 37°C in a 5% CO_2 , humid atmosphere. Cells were identified as endotheliocytes by their typical cobblestone appearance under optical microscopy, and by the presence of Von Willebrand factor as visualised by immunofluorescence (not shown). Cell cultures were used before the 8th passage, in order to avoid degeneration and apoptosis as induced by subculture and senescence.

Primary cultures of human cardiac microvascular endothelial (HMVEC-c) cells (a kind gift of Prof. Marco Arese, Institute for Cancer Research and Treatment, Candiolo, Italy) were maintained in EGM-2MV endothelial growth medium containing supplements provided by the supplier (Cambrex Biosciences, Walkersville, MD).

Porcine large artery endothelial cells (PAOEC), derived from plaque free porcine aorta, were obtained from the European Collection of Cell Cultures (ECACC). PAOEC were maintained in DMEM (high glucose, 4.5 g/L), supplemented with 10% FBS, 2% L-glutamine (200 mM), 100 U/ml penicillin and 100 $\mu\text{g}/\text{ml}$ streptomycin.

Brain endothelial cells (bEnd5), derived from mouse brain endothelium, were a kind gift from Prof. Laura Riboni (University of Milan). bEnd5 were grown in DMEM (high glucose, 4.5 g/L), supplemented with 10% FBS, 1% non-essential amino acid (10 mM), 1% sodium pyruvate (100 mM), 2% L-glutamine (200 mM), 100 U/ml penicillin and 100 $\mu\text{g}/\text{ml}$ streptomycin.

The PL was obtained as described by Ranzato et al. [2008, 2009b]. Briefly, platelet concentrates were derived by platelet aphaeresis collection from blood samples of single volunteer donors after informed consent. Platelet concentrates were centrifuged, washed, repeatedly frozen and thawed to obtain the PL, centrifuged to eliminate debris, and stored at -80°C until use.

CRYSTAL VIOLET (CV) AND NEUTRAL RED UPTAKE (NRU) ASSAYS

Cell proliferation was assessed by staining cells with the CV dye. Each well contained about 20,000 cells in a total volume of 100 μl of DMEM with 10% FBS. Cells were incubated with PL at various concentrations for 24 h. The medium was then removed, cells were gently washed once with $1\times$ PBS, stained for 10 min with 0.5% CV in 145 mmol/L NaCl, 0.5% formal saline, 50% ethanol, and washed thrice with water. CV was eluted from cells with 33% acetic acid and the absorption of the supernatant was measured at 540 nm in a plate reader (Sirio S, SEAC, Florence, Italy).

For NRU assay, cells were seeded on 96-well plates (20,000 cells/well), grown overnight in DMEM with 10% FBS, and exposed to PL as above. After removing the medium, a 0.05% solution of neutral red was added to each well, followed by incubation for 3 h at 37°C. Cells were then washed with $1\times$ PBS, followed by the addition of a solution of 1% glacial acetic acid in 50% ethanol, in order to fix the cells and extract the neutral red dye incorporated into the lysosomes. Thereafter, plates were shaken and the absorbance was measured at 540 nm.

SCRATCH WOUND AND CHEMOTAXIS ASSAY

Scratch wounds were created in confluent cell monolayers growing in 12-well plates by using a sterile 0.1–10 μl pipette tip. After washing away suspended cells, cultures were refed with medium in the presence or absence of 20% PL. Thereafter, at 0, 6 or 24-h post-wounding, cells were fixed in 3.7% formaldehyde in PBS for 30 min, and then stained with 0.1% toluidine blue at room temperature for 30 min. Cell migration into the wound space was estimated at 0 and 24 h after wounding with image analysis, by using an inverted Televel microscope (Carl Zeiss, Inc., Thornwood, NY) equipped with a digital camera. Wound closure was determined as the difference between wound width at 0 and 24 h.

A chemotaxis assay was performed on HuVEC in transwell plates (8 μm pore size, Pbi International, Milan, Italy). A total of 1×10^5 cells per well were seeded in the upper compartment of filters, while 20% PL was added to the lower compartment. After 24 h incubation, filters were removed and stained with 0.5% CV (145 mmol/L NaCl, 0.5% formal saline, 50% ethanol) for 10 min and washed thrice with

water. The upper side of filters was scraped using a cotton swab to remove cells that had attached but not migrated. Following PBS washing of filters, the dye was eluted from cells with 33% acetic acid, and measured at 540 nm.

INTRACELLULAR CALCIUM MEASUREMENTS

HuVEC cells were plated on glass-base dishes (Iwaki Glass, Inc., Tokyo, Japan), allowed to settle overnight, and then loaded in the dark at 4°C for 60 min with the cell-permeant, fluorescent calcium probe fluo-3/AM (20 μM) in a loading buffer consisting of (mM) 10 HEPES, 140 NaCl, 10 glucose, 1 MgCl₂, 2 CaCl₂, 5 KCl, pH 7.4. For Ca²⁺-free experiments, Ca²⁺ was omitted from the loading buffer. After probe loading and washing, cells were examined through confocal time-lapse analysis at 21°C, using a Zeiss LSM 510 confocal system interfaced with a Zeiss Axiovert 100 M microscope (Carl Zeiss, Inc.). Excitation was obtained by the 488 nm line of an Ar laser, and emission was collected using a 505–550 bandpass filter. The laser power was reduced to 15% in order to lower probe bleaching. Confocal imaging was performed with a resolution of 512 × 512 pixels at 256 intensity values, with a framing rate of 1 frame/20 s. Several cells were viewed together through a 20× Plan-Neofluar Zeiss objective (0.5 NA). Fluo-3 fluorescence was measured in digitised images as the average value over defined contours of individual cells, using the ROI-mean tool of the Zeiss LSM 510 2.01 software. Fluo-3 calibration was achieved by the equation [Grynkiewicz et al., 1985]:

$$[Ca^{2+}]_i = K_d(F - F_{min}) / (F_{max} - F)$$

where $K_d = 400$ nM, while F_{max} and F_{min} are maximum and minimum fluorescence intensities, measured after cell treatment with 200 μM A23187 and 2.0 mM EGTA, respectively.

WESTERN BLOT

HuVEC cells allowed to grow in 12-well plates were subjected to multiple scratch wounding (two couples of perpendicularly oriented wounds) in the presence or absence of 20% PL for 5, 15, 30 and 60 min, and then lysed in Laemmli buffer [Laemmli, 1970]. Amounts of 20 μg of protein were loaded on gel, subjected to SDS-PAGE (12% gel) and transferred to a nitrocellulose membrane using a Bio-Rad Mini Trans Blot electrophoretic transfer unit. The membranes were blocked for non-specific protein with 5% non-fat, dry milk in PBS and then probed at room temperature for 1 h, or at 4°C overnight, with specific primary antibodies (1:1,000, Cell Signaling Technology, Celbio SpA, Milan, Italy) against p-ERK1/2, p-p38, p-AKT, ERK1/2, p38 and AKT. Membranes were then washed three times (10 min per wash) with PBS containing 0.05% Tween-20, to remove unbound antibodies, and then further incubated with appropriate horseradish-peroxidase-conjugated secondary antibodies (1:1,000). Membranes were developed by an ECL kit (Millipore, Billerica, MA), according to the manufacturer's protocol, digitised with the Quantity One Image Software (ChemIDoc XRS, Bio-Rad Laboratories, Hercules, CA) and normalised against proper loading controls. Band intensities were quantified by densitometric analysis using the Adobe Photoshop 7.0.1 software (Adobe Systems, Inc., San Jose, CA).

STATISTICS

Data were analysed by ANOVA, and by the Tukey's and the Dunnett's tests, using the InStat software package (GraphPad Software, Inc, San Diego, CA).

RESULTS

CELL PROLIFERATION AND VIABILITY

The effects of increasing PL concentrations (1–100%, v/v) on endothelial cell proliferation and viability were explored by using the CV and NRU assays. Data showed that PL produces no toxicity up to a dose as high as 50%. Evidence of significant toxicity was only found at 100% PL, on PAOEC with CV, and on bEnd5 with NRU (Fig. 1). In addition, the treatments induced variable increases of cell viability and proliferation, with maximum effects observed at 20% PL. The highest stimulatory effect was recorded in HMVEC-c, as shown by CV data (Fig. 1). Based on these results, we decided to perform the following experiments by using a concentration of 20% PL.

SCRATCH WOUND REPAIR

Scratch wounded endothelial cells incubated in the presence of PL showed significantly higher wound closure rates with respect to controls (Fig. 2). The measurements of wound closure rate showed a significant increase in the presence of 20% PL at both 6 and 24 h in all cell types (Fig. 3). However, HuVEC cells showed the strongest response to PL, particularly at 6 h after scratching. Such a result led us to choose HuVEC in order to investigate the role played by cell signalling pathways in the PL effect on wound closure.

We therefore performed scratch wound experiments at 6 h on HuVEC by using the following kinase inhibitors: PD98059 (MEK1/2 inhibitor preventing ERK1/2 activation, 10 μM), SB203580 (p38 inhibitor, 20 μM), wortmannin (PI3K inhibitor, 500 nM) and the cell-permeant, Ca²⁺ chelator BAPTA-AM (30 μM). Confluent cells were scratched in the absence or presence of each inhibitor, with or without PL, and wound closure was then measured at 6 h post-wounding. In the absence of PL, inhibitors did not alter wound closure rates respect to control, whereas they affected the increase of wound closure rate induced by PL. PD98059 exerted the highest inhibitory effects, BAPTA-AM exerted an intermediate inhibitory effect, while wortmannin and SB203580 were less effective (Fig. 4A). The effect of the vehicle alone (0.1% DMSO) was negligible, either in the presence or absence of PL (not shown).

CELL CHEMOTACTIC RESPONSE

In order to assess whether PL can influence cell migration rates, we subjected HuVEC cells to a chemotaxis assay performed with 8 μm polycarbonate transwell filters (Fig. 4B). In this set of experiments, the inhibitors used in scratch wound assays were also used (except for BAPTA-AM). In the presence of PL and in the absence of inhibitors, the number of migrating cells was significantly increased respect to control ($P < 0.01$). By contrast, all inhibitors totally abrogated the effect of PL on cell migration ($P < 0.01$). The vehicle alone caused no variations with respect to control (not shown).

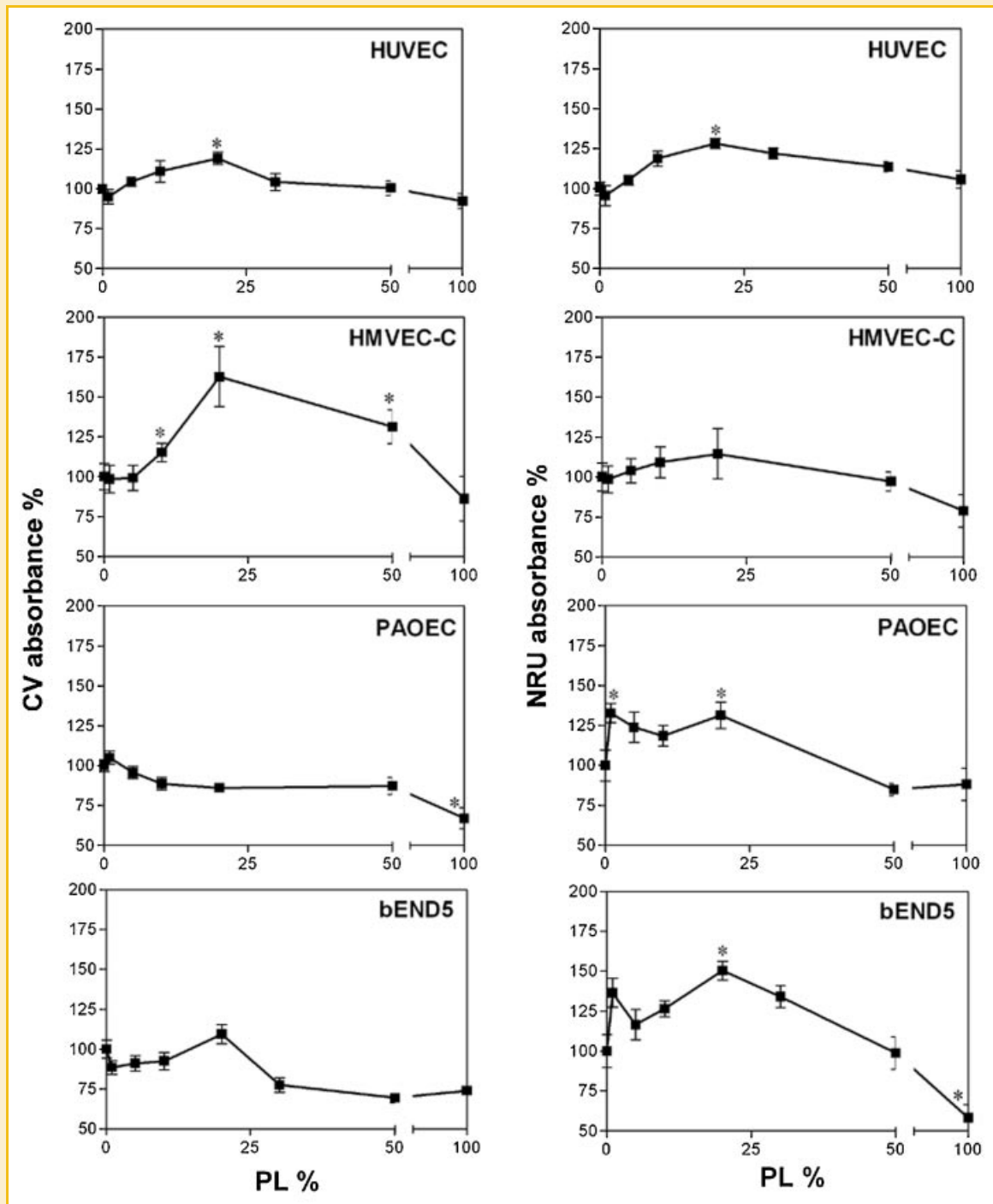


Fig. 1. Cell proliferation and viability of endothelial cells exposed to increasing concentrations of PL and evaluated by the CV and NRU cytotoxicity assays. Data are expressed as means \pm SD of absorbances ($n = 12$ from two independent experiments) (see the Materials and Methods Section for further details). The means of control has been set to 100%. * Significantly different with respect to control according to the Dunnett's test ($P < 0.01$).

CALCIUM SIGNALLING

Confocal Ca^{2+} imaging of HuVEC cells showed the induction of Ca^{2+} dynamics immediately after exposure to 20% PL. These Ca^{2+} signals occurred in the majority of cells, showing complex patterns and variable intensities among cells. Time courses of intracellular Ca^{2+} variation derived from confocal imaging showed stable values under

control conditions, while PL exposure triggered Ca^{2+} dynamics lasting for about 10–15 min (Fig. 5A). The analysis of single cells revealed the occurrence of a series of Ca^{2+} spikes, each lasting about 15–20 s, whose frequency showed a maximum immediately after PL exposure and then tended to decrease, until Ca^{2+} oscillations disappeared after 10–15 min (Fig. 5B). In the absence of external Ca^{2+} these spikes were

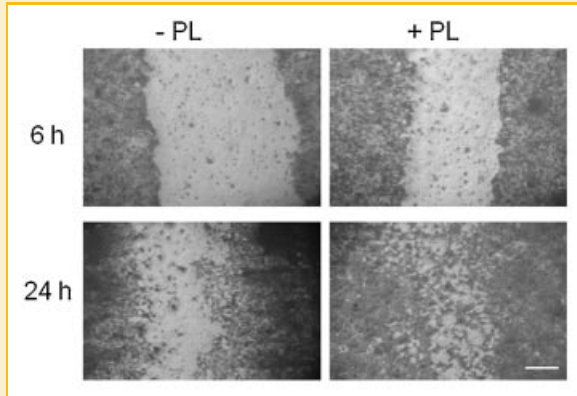


Fig. 2. Phase contrast micrographs of wound scratched HuVEC cells that were fixed and stained with blue-toluidine at 6 or 24 h after scratching, in the presence or absence of 20% PL. Scale bar: 300 μm .

still visible, although showing on the average lower amplitudes. Taken together, these findings suggest an involvement of Ins3P-dependent intracellular Ca^{2+} release.

PROTEIN PHOSPHORYLATION SIGNALLING

In order to explore the role of phosphorylation cascades in endothelium repair, the activation of p38 and ERK1/2 MAP kinases, and of the PI3K-dependent kinase Akt, were examined by Western blotting at 5, 15, 30 and 60 min post-wounding. These analyses were carried out by using antibodies against the total forms of the two MAPKs and Akt, and against their phosphorylated forms. Scratch wound per se did not induce any detectable activation of these kinases, with the exception of a slight activation trend of Akt (Fig. 6). The p38 MAP kinase showed the highest baseline phosphorylation level, but in the presence of PL no further activation was visible, whereas there was instead a slight decrease starting from 30 min after wounding. In contrast, exposure to PL induced a marked activation of Akt, which lasted for about 15 min. ERK1/2 also showed PL-induced activation but with a completely different pattern, consisting in a sustained phosphorylation that started at 15 min after wounding and lasted for at least 60 min (Fig. 6).

Given the sustained activation of ERK1/2 in the PL-induced cell signalling, we also investigated the role played by this MAPK in the cell proliferation effect. Cells were exposed for 24 h to PL in the presence or absence of PD98059 and cell proliferation was assessed by the CV test. Data showed that PD98059 did not inhibit basal proliferation, but fully inhibited the increase in proliferation rate induced by PL, as assessed through the Tukey's post hoc multiple test (Fig. 7). In addition, two-way ANOVA showed significant effects of PL and PD98059 taken separately ($P < 0.01$), but no significant correlation between them ($P > 0.05$), thus confirming that PD98059 inhibited PL-induced proliferation rates but not basal rates.

In order to obtain further confirmation about the role of ERK1/2 in mediating the effects of PL, we used U0126, another MEK1/2 inhibitor structurally unrelated with PD98059. The results obtained

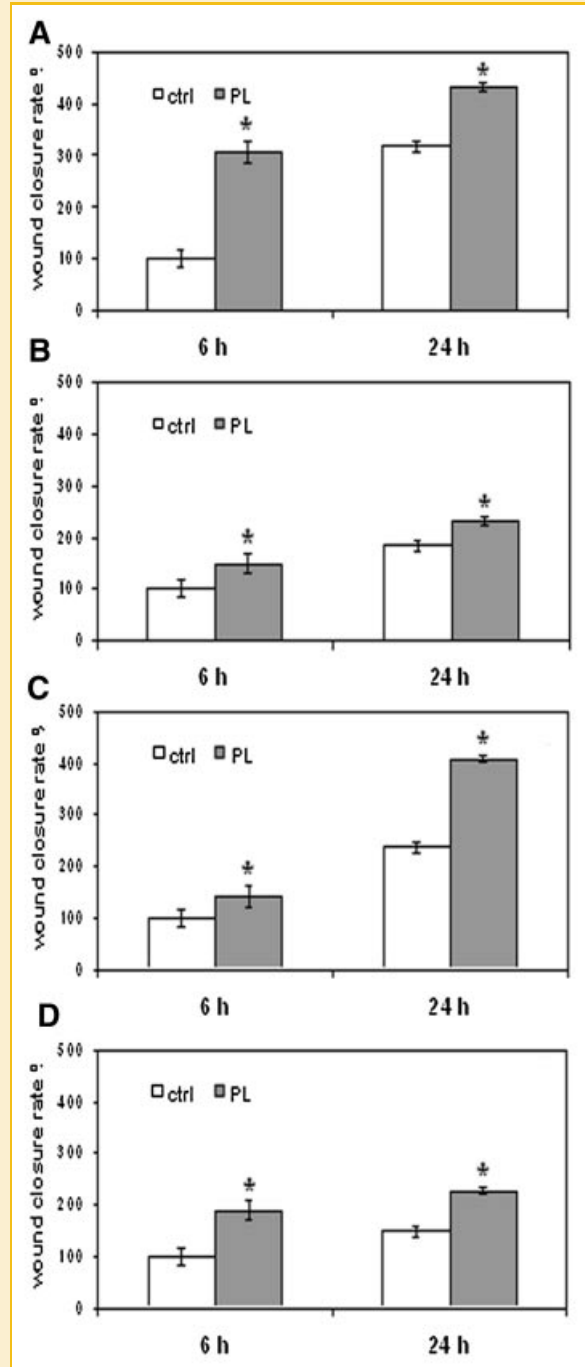


Fig. 3. Effects of 20% PL on scratch wound healing of confluent endothelial cells (A: HuVEC; B: HMVEC-C; C: PAOEC; D: bEnd5). Each bar represents the mean \pm SD ($n = 20$) of wound closure rates expressed as the difference between wound width at 0 h and at 6 or 24 h. The means of control rates at 6 h has been set to 100%. * Significantly different with respect to control ($P < 0.01$).

with U0126 were quite similar to those obtained with PD98059: U0126 suppressed both the proliferatory and the chemotactic effect of PL, while the acceleration of wound closure rate induced by PL was significantly reduced (Fig. 8).

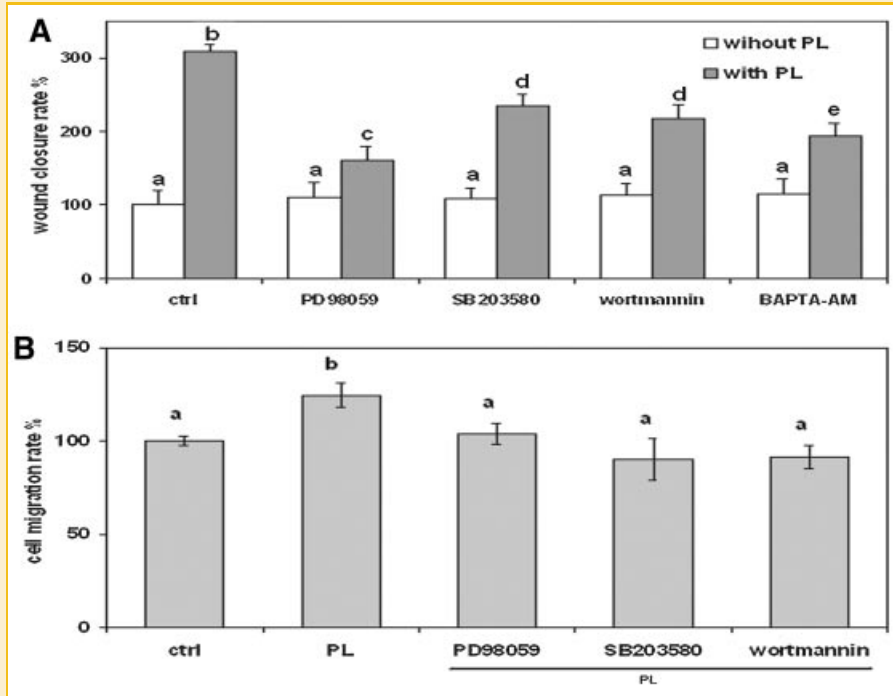


Fig. 4. A: Effect of different inhibitors on scratch wound repair of confluent HuVEC cells. Data were recorded 6 h after wounding of cells exposed or not to 20% PL, in the presence or absence of various drugs. Each bar represents the mean \pm SD ($n = 20$) of wound closure rates expressed as in Figure 3. The mean of controls without PL has been set to 100%. Different letters on bars indicate significant differences according to the Tukey's test ($P < 0.01$). B: Effects of PL and of different inhibitors on transwell cell migration (see the Materials and Methods Section). Data are means \pm SD of the numbers of migrating cells evaluated by cell staining with crystal violet, followed by dye elution and measurement of absorbance at 540 nm ($n = 5$). The mean of controls has been set to 100%. Statistics as above.

DISCUSSION

Platelets contain a series of factors able to influence cellular activities at wounded sites, including growth factors, cytokines and chemokines. We used HuVEC cells as a main experimental model given their high growth rate and optimal response to PL. However, platelets contain high levels of factors that activate PDGFR and CXCR3R, two receptors reported to be only negligibly expressed in HuVEC [Gupta et al., 1998], but at functional levels in human microvascular cells [Beitz et al., 1991; Romagnani et al., 2001]. Hence, we confirmed the key experiments of this study in human microvascular cells, and also included in the study non-human vascular models, in order to obtain a wider panel of data about the potentialities of PL factors in the stimulation of wound healing.

The CV assay highlighted a mitogenic effect of PL, thus confirming previous findings about cell proliferation induced by PL on different cell types [Ranzato et al., 2008, 2009b]. Interestingly, the proliferative effect of PL was maximum in microvascular HMVEC-c cells, in which the expression of PDGFR and CXCR3 has been characterised. Moreover, scratch wound data showed that PL induces a marked increase in the wound repair capabilities of endothelial cells, but in this case the strongest response was recorded for HuVEC, in which the expression of PDGFR and CXCR3 does not seem to occur. Hence, our data suggest that the induction of wound healing by PL depends on a complex of effects, possibly involving both cell proliferation and locomotory behaviour. Such a view is

supported by data from the cell migration assay, which showed a chemoattractant activity of PL on HuVEC. These data confirm previous findings about the chemotactic responses to platelet derivatives of retinal glial cells [Castelnuovo et al., 2000], rat foetal cells [Soffer et al., 2003], mature osteoblasts [Celotti et al., 2006], keratinocytes [Ranzato et al., 2008] and primary fibroblasts [Ranzato et al., 2009b].

Cytosolic free Ca^{2+} is essential for cell proliferation and motility [Cheng et al., 2006], and its role in wound healing has been repeatedly described. Studies carried out on endothelial cells have shown wound-induced Ca^{2+} waves [Berra-Romani et al., 2008], while intracellular Ca^{2+} rises have been found to stimulate cell growth and movement during endothelial repair [Sammak et al., 1997; Ehring et al., 2000]. It has been also shown that Ca^{2+} rises lead to nitric oxide production, which in turn promotes endothelial cell proliferation [Erdogan et al., 2005]. A correlation between Ca^{2+} dynamics and wound repair has been also reported in studies on skin cells, where PL has induced noticeable Ca^{2+} signals, and BAPTA-AM has abolished the PL effect on wound healing [Ranzato et al., 2008, 2009b]. In our experiments, the role of cell Ca^{2+} in HuVEC endothelial repair was revealed by the inhibitory effect on PL of the Ca^{2+} chelator BAPTA-AM. In addition, confocal Ca^{2+} imaging showed PL-induced Ca^{2+} oscillations that were partially independent from extracellular Ca^{2+} and showed the typical aspect of InsP₃-controlled, frequency-encoded Ca^{2+} signalling. Such a result is quite in line with the notion that InsP₃ formation and calcium

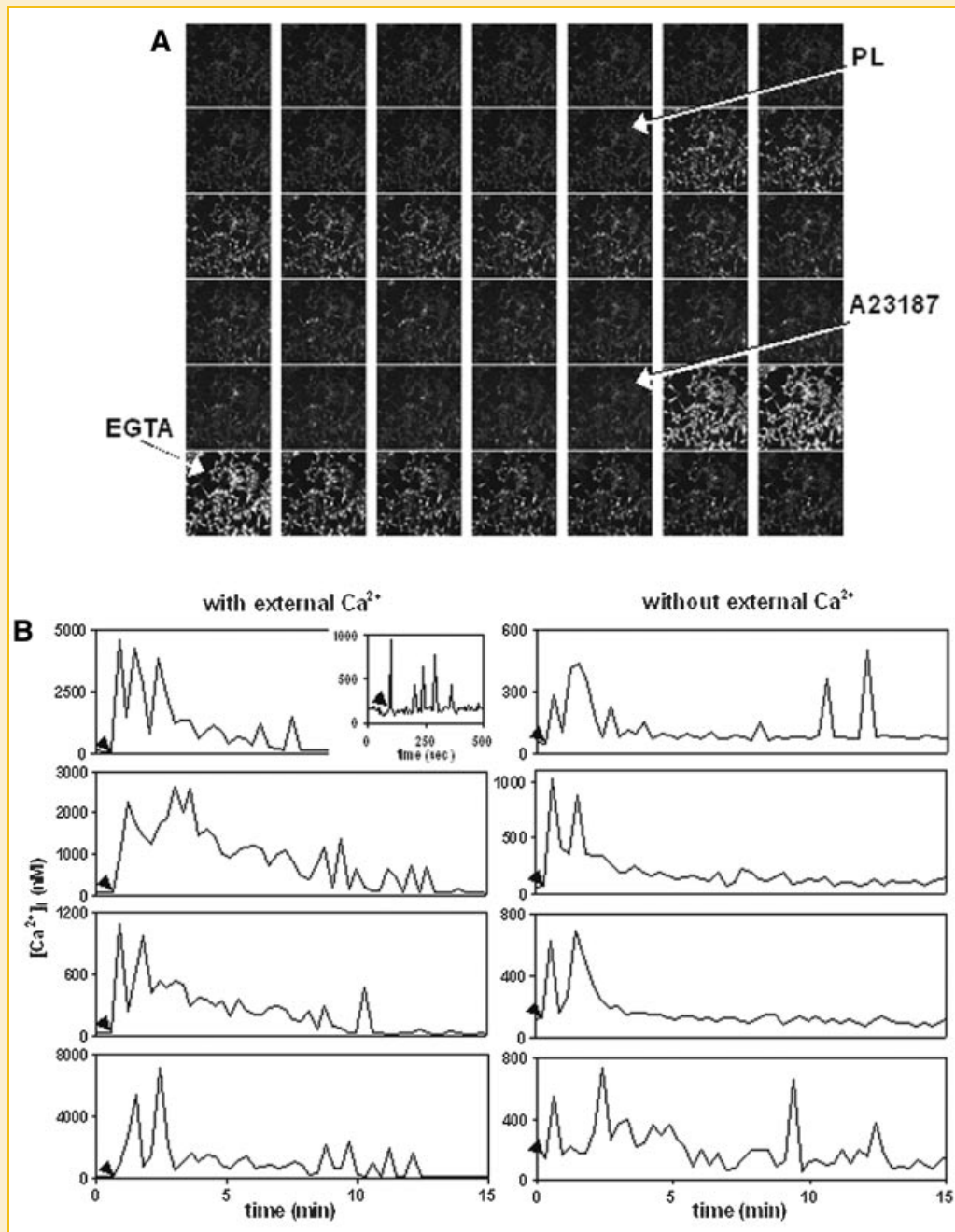


Fig. 5. A: Confocal Ca^{2+} imaging of HuVEC loaded with the fluo-3 probe and exposed to PL. Time lapse confocal images (field size, $450 \mu\text{m} \times 450 \mu\text{m}$) were acquired at 1-min intervals, showing that PL (20%) induces transient intracellular Ca^{2+} rise in a number of cells. At the end of the experiments, Ca^{2+} probe calibration was carried out by exposing cells to $200 \mu\text{M}$ A23187, followed by 2.0 mM EGTA. B: Traces of intracellular Ca^{2+} variations recorded by confocal imaging in individual HuVEC cells after addition of 20% PL (arrowheads). The traces of each column are representative of about 50 cells. In the presence of external Ca^{2+} (left column), cell responses are characterised by Ca^{2+} spikes, which tend to decrease in both frequency and amplitude, until they disappear at about 15 min since exposure. A more detailed Ca^{2+} trace shows that each spike lasts about 15–20 s (inset). In the absence of external Ca^{2+} (right column), PL induces a similar pattern of Ca^{2+} oscillations but with lower frequencies and amplitudes.

mobilisation are typical cellular responses to serum growth factors [Berridge et al., 1984]. The strong Ca^{2+} signals provoked in HuVEC cells by PL could in part explain the sustained activation of ERK1/2, since it is known that intracellular Ca^{2+} rises can activate this MAP kinase through different mechanisms [Agell et al., 2002; Cullen and Lockyer, 2002; Schmitt et al., 2004].

In various cell types, it has been found that ERK1/2 and p38 MAPKs become activated by tissue wounding [Cole et al., 2001; Leiper et al., 2006]. ERK1/2, JNK and p38 have been implicated in the vascular response to injury, such as balloon injury of rat carotid artery or thoracic aorta [Bishara et al., 2002; Ambudkar et al., 2007]. Our Western blot analyses showed that p38 was not activated by PL, but

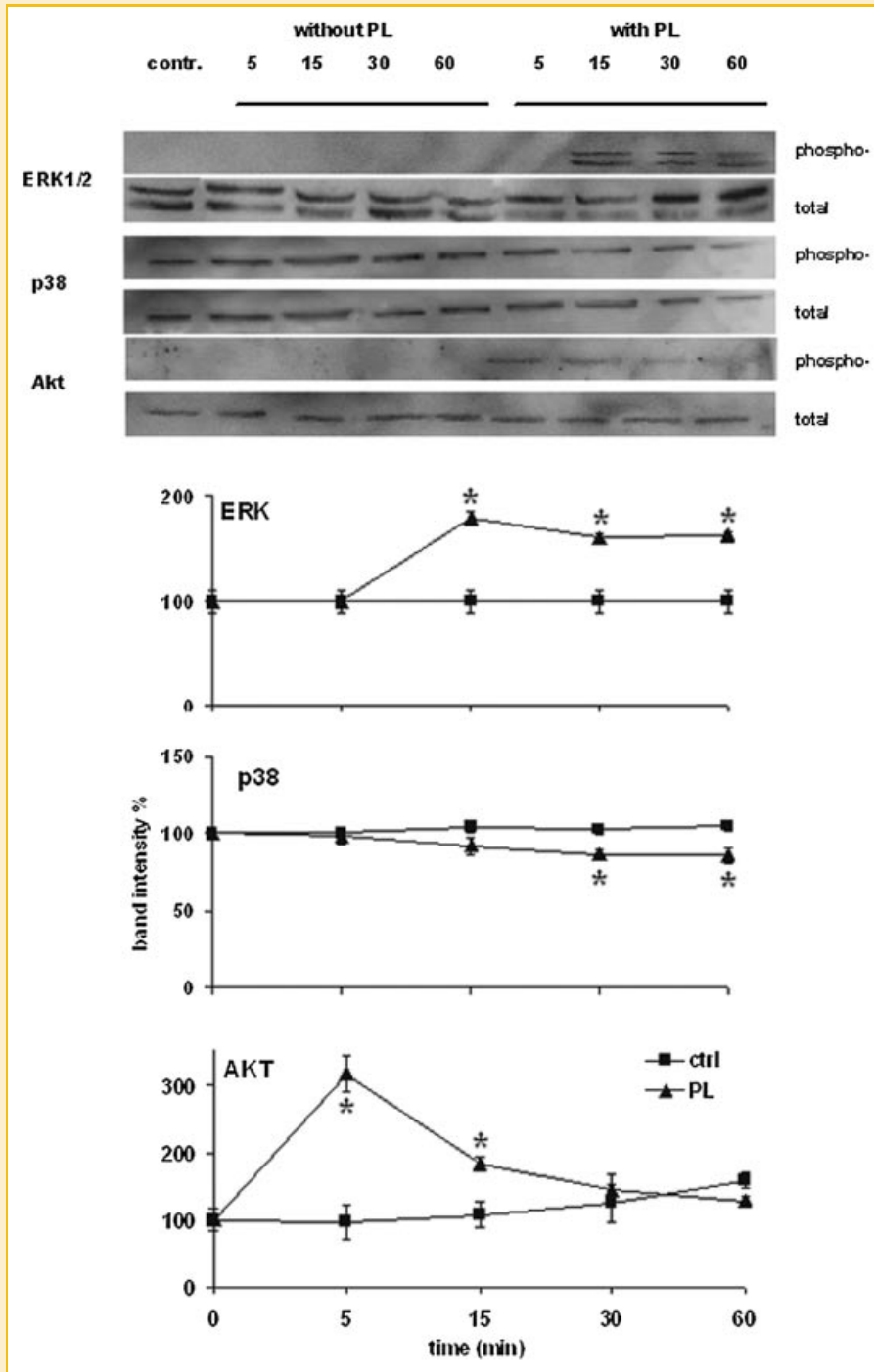


Fig. 6. Effect of PL on the activation of ERK1/2, p38 and Akt after multiple scratch wounding of HuVEC monolayers. Upper panels: Total cell lysates (20 μ g protein/lane) obtained from wounded cells were separated on 12% SDS-PAGE, transferred to a nitrocellulose membrane, labelled with anti-phospho-ERK1/2, -phospho-p38 or -phospho-Akt, and then stripped and reprobbed with anti-ERK1/2, -p38 or -Akt as internal controls. Lower panels: Time courses of ERK1/2, p38, and Akt activation within 60 min after wounding. Data are means \pm SD (n = 3) of the ratio between the optical densities of the bands of the phosphorylated form and of the corresponding total protein. The means of controls have been set to 100%. * $P < 0.01$, with respect to time $t = 0$, according to the Dunnett's test.

instead it underwent a slightly dephosphorylation, while concurrently, we observed a sustained activation of ERK1/2. These two events are most likely correlated, since in some cases a seesaw-like balance between p38 and ERK1/2 phosphorylation has been observed,

suggesting a fine-tuned cross talk between these two MAP kinases [Liu and Hofmann, 2004]. It has been found, in particular, that ERK1/2 activation by TGF- β , a platelet-derived cytokine, upregulates MAPK phosphatase 1, thereby inactivating p38 [Xiao et al., 2002].

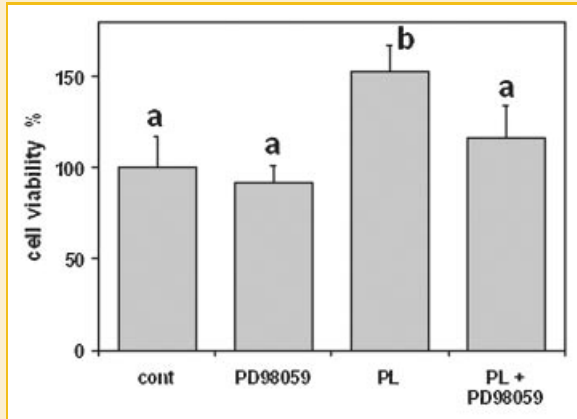


Fig. 7. Effect of 20% PL and of 10 μ M PD98059 on HuVEC cell proliferation evaluated by the CV test after 24 h of treatment. Data are expressed as means \pm SD of absorbances ($n=8$), and the mean of control has been set to 100%. Cont: no treatment; PD98059: exposure to PD98059 only; PL: exposure to PL only; PL + PD98059: exposure to both. Different letters on bars indicate significant differences according to the Tukey's test ($P < 0.01$).

The PI3K/Akt signalling pathway has also been reported to play a role in the wound healing of different cell types [Miura et al., 2003; Xu et al., 2004; Buffin-Meyer et al., 2007; Ranzato et al., 2009b], while in endothelial cells this pathway is known to mediate cell survival, proliferation, migration, and angiogenesis [reviewed in Shiojima and Walsh, 2002]. However, in the presence of PL, Akt underwent a transient activation, whereas ERK1/2 showed long-lasting activation. Such a result was quite in line with the fact that two inhibitors of ERK1/2 activation, namely PD98059 and U0126, suppressed PL-induced cell proliferation and exerted the strongest inhibition on PL-induced wound healing. Hence, different data concur to indicate that in HuVEC the mechanism of action of PL is mostly controlled by ERK1/2.

In conclusion, this study has demonstrated that PL activates repair mechanisms in various types of injured endothelial cell layers. These data bring scientific support to possible clinical applications of platelet derivatives in blood vessel repair, and in particular to the functionalisation of biomaterials used in tissue engineering. These latter techniques have already shown strong potentials for the treatment of chronic wounds [Naughton and Mansbridge, 1999], burns [Kopp et al., 2004] and cartilage defects [Angele et al., 2004]. However, scaffolds used in tissue engineering are frequently driven by hydrophobic materials that lower cell affinity and permeation by nutrient fluids [Whang et al., 2000]. These drawbacks can be overcome through the design of biomimetic materials capable of directing new tissue formation, and since some results have already been obtained with growth factors [Bowen-Pope et al., 1984; Boccafoschi et al., 2005], platelets have also started to be employed as a growth factor source in these techniques [Chang et al., 2007]. Hence, the implementation of platelet derivatives in biomaterials could offer innovative solutions to blood vessel engineering.

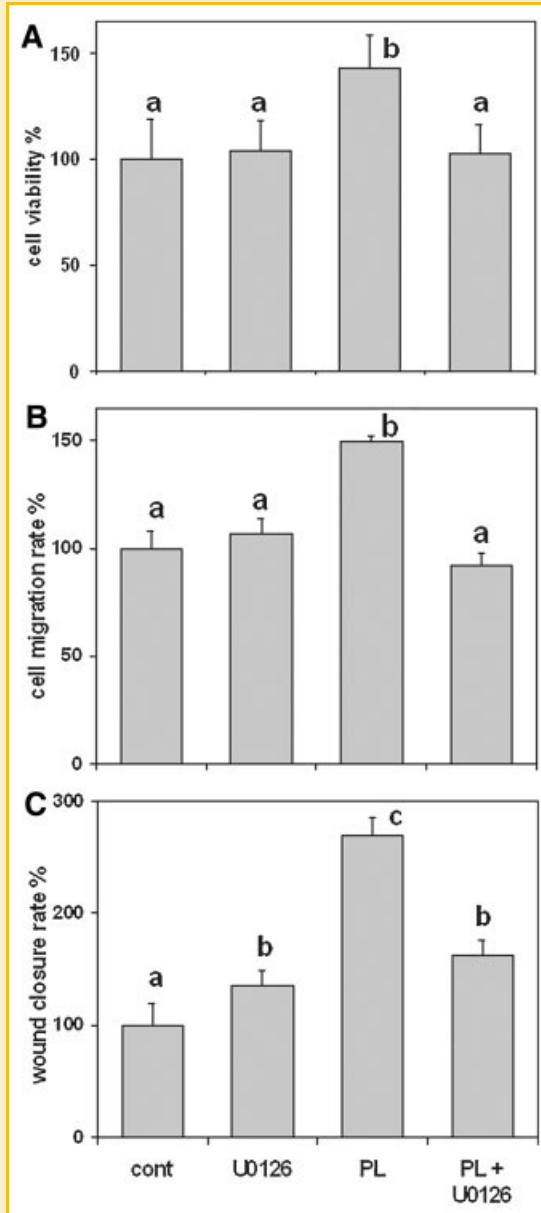


Fig. 8. Suppressive effects of the ERK1/2 inhibitor U0126 (10 μ M) on the induction of cell proliferation (A), cell migration (B) and wound healing acceleration (C) exerted by 20% PL on HuVEC cells. A: Data from the CV test are expressed as means \pm SD of absorbances ($n=6$). B: Data are means \pm SD ($n=5$) of the numbers of migrating cells evaluated by a transwell assay as reported in Figure 4B. C: Data are means \pm SD ($n=25$) of wound closure rates expressed as in Figure 3. In all graphs the mean of control has been set to 100%. Different letters on bars indicate significant differences according to the Tukey's test ($P < 0.01$).

ACKNOWLEDGMENTS

This work was supported by a grant from Ricerca Sanitaria Finalizzata, Regione Piemonte, Italy, 2008, and by grants from the University of Piemonte Orientale "Amedeo Avogadro". ER is recipient of a Research Fellowship from the University of Piemonte Orientale.

REFERENCES

- Agell N, Bachs O, Rocamora N, Villalonga P., 2002. Modulation of the Ras/Raf/MEK/ERK pathway by Ca(2+), and calmodulin. *Cell Signal* 14: 649–654.
- Ambudkar IS, Ong HL, Liu X, Bandyopadhyay BC, Cheng KT. 2007. TRPC1: The link between functionally distinct store-operated calcium channels. *Cell Calcium* 42:213–223.
- Angele P, Abke J, Kujat R, Faltermeier H, Schumann D, Nerlich M, Kinner B, Englert C, Ruzszzak Z, Mehrl R, Mueller R. 2004. Influence of different collagen species on physico-chemical properties of crosslinked collagen matrices. *Biomaterials* 25:2831–2841.
- Beitz JG, Kim IS, Calabresi P, Frackelton AR. 1991. Human microvascular endothelial cells express receptors for platelet-derived growth factor. *Proc Natl Acad Sci USA* 88:2021–2025.
- Berra-Romani R, Raqeeb A, Velino-Cruz JE, Moccia F, Oldani A, Speroni F, Taglietti V, Tanzi F. 2008. Ca²⁺ signaling in injured in situ endothelium of rat aorta. *Cell Calcium* 44:298–309.
- Berridge MJ, Heslop JP, Irvine RF, Brown KD. 1984. Inositol trisphosphate formation and calcium mobilization in Swiss 3T3 cells in response to platelet-derived growth factor. *Biochem J* 222:195–201.
- Bishara NB, Murphy TV, Hill MA. 2002. Capacitative Ca(2+) entry in vascular endothelial cells is mediated via pathways sensitive to 2 aminoethoxydiphenyl borate and xestospongins. *Br J Pharmacol* 135:119–128.
- Boccafroschi F, Habermehl J, Vesentini S, Mantovani D. 2005. Biological performances of collagen-based scaffolds for vascular tissue engineering. *Biomaterials* 26:7410–7417.
- Bowen-Pope DF, Malpass TW, Foster DM, Ross R. 1984. Platelet-derived growth factor in vivo: Levels, activity, and rate of clearance. *Blood* 64:458–469.
- Buffin-Meyer B, Crassous PA, Delage C, Denis C, Schaak S, Paris H. 2007. EGF receptor transactivation and PI3-kinase mediate stimulation of ERK by alpha(2A)-adrenoreceptor in intestinal epithelial cells: A role in wound healing. *Eur J Pharmacol* 574:85–93.
- Castelnuovo L, Dosquet C, Gaudric A, Sahel J, Hicks D. 2000. Human platelet suspension stimulates porcine retinal glial proliferation and migration in vitro. *Invest Ophthalmol Vis Sci* 41:601–609.
- Celotti F, Colciago A, Negri-Cesi P, Pravettoni A, Zaninetti R, Sacchi MC. 2006. Effect of platelet-rich plasma on migration and proliferation of SaOS-2 osteoblasts: Role of platelet-derived growth factor and transforming growth factor-beta. *Wound Repair Regen* 14:195–202.
- Chang T, Liu Q, Marino V, Bartold PM. 2007. Attachment of periodontal fibroblasts to barrier membranes coated with platelet-rich plasma. *Aust Dent J* 52:227–233.
- Cheng HP, Wie S, Wie LP, Verkhatsky A. 2006. Calcium signaling in physiology and pathophysiology. *Acta Pharmacol Sin* 27:767–772.
- Cole J, Tsou R, Wallace K, Gibran N, Isik F. 2001. Comparison of normal human skin gene expression using cDNA microarrays. *Wound Repair Regen* 9:77–85.
- Cullen PJ, Lockyer PJ., 2002. Integration of calcium and Ras signalling. *Nat Rev Mol Cell Biol*. 3:339–348.
- Ehring GR, Szabo IL, Jones MK, Sarfeh IJ, Tarnawski AS. 2000. ATP-induced Ca²⁺-signaling enhances rat gastric microvascular endothelial cell migration. *J Physiol Pharmacol* 51:799–811.
- Erdogan A, Schaefer CA, Schaefer M, Luedders DW, Stockhausen F, Abdallah Y, Schaefer C, Most AK, Tillmanns H, Piper HM, Kuhlmann CR. 2005. Margatoxin inhibits VEGF-induced hyperpolarization, proliferation and nitric oxide production of human endothelial cells. *J Vasc Res* 42:368–376.
- Giusti I, Rugghetti A, D'Ascenzo S, Millimaggi D, Pavan A, Dell'Orso L, Dolo V. 2009. Identification of an optimal concentration of platelet gel for promoting angiogenesis in human endothelial cells. *Transfusion* 49:771–778.
- Gotlieb AI. 1997. Endothelial regulation of vascular repair: Role of bFGF in paracrine pathways. *Endocr Pathol* 2:129–135.
- Gryniewicz G, Poenie M, Tsien RY. 1985. A new generation of Ca²⁺-indicators with greatly improved fluorescence properties. *J Biol Chem* 260:3440–3450.
- Gupta SK, Lysko PG, Pillarisetti K, Ohlstein E, Stadel JM. 1998. Chemokine receptors in human endothelial cells. Functional expression of CXCR4 and its transcriptional regulation by inflammatory cytokines. *J Biol Chem* 273: 4282–4287.
- Jaffe EA, Nachman RL, Becker CG, Minick CR. 1973. Culture of human endothelial cells derived from umbilical veins. Identification by morphologic and immunologic criteria. *J Clin Invest* 52:2745–2756.
- Kopp J, Jeschke MG, Bach AD, Kneser U, Horch RE. 2004. Applied tissue engineering in the closure of severe burns and chronic wounds using cultured human autologous keratinocytes in a natural fibrin matrix. *Cell Tissue Bank* 5:89–96.
- Laemmli UK. 1970. Cleavage of structural proteins during the assembly of the head of bacteriophage T4. *Nature* 227:680–685.
- Leiper LJ, Walczysko P, Kucerova R, Ou J, Shanley LJ, Lawson D, Forrester JV, McCaig CD, Zhao M, Collinson JM. 2006. The roles of calcium signaling and ERK1/2 phosphorylation in a Pax6+/- mouse model of epithelial wound-healing delay. *BMC Biol* 4:27.
- Liu Q, Hofmann PA., 2004. Protein phosphatase 2A-mediated cross-talk between p38 MAPK and ERK in apoptosis of cardiac myocytes. *Am J Physiol Heart Circ Physiol*. 286:2204–2212.
- Martin P. 1997. Wound healing: Aiming for perfect regeneration. *Science* 276:75–81.
- Mazzucco L, Medici D, Serra M, Panizza R, Rivara G, Orecchia S, Libener R, Cattana E, Levis A, Betta PG, Borzini P. 2004. The use of autologous platelet gel to treat difficult-to-heal wounds: A pilot study. *Transfusion* 44:1013–1018.
- Miura Y, Yanagihara N, Imamura H, Kaida M, Moriwaki M, Shiraki K, Miki T. 2003. Hepatocyte growth factor stimulates proliferation and migration during wound healing of retinal pigment epithelial cells in vitro. *Jpn J Ophthalmol* 47:268–275.
- Naughton GK, Mansbridge JN. 1999. Human-based tissue-engineered implants for plastic and reconstructive surgery. *Clin Plast Surg* 26:579–586.
- Ovington LG. 2007. Advances in wound dressings. *Clin Dermatol* 25:33–38.
- Ranzato E, Balbo V, Boccafroschi F, Mazzucco L, Burlando B. 2009a. Scratch wound closure of C2C12 mouse myoblasts is enhanced by human platelet lysate. *Cell Biol Int* 33:911–917.
- Ranzato E, Mazzucco L, Patrone M, Burlando B. 2009b. Platelet lysate promotes in vitro wound scratch closure of human dermal fibroblasts: Different roles of cell calcium, p38, ERK, and PI3K/ Akt. *J Cell Mol Med* 8b:2030–2038.
- Ranzato E, Patrone M, Mazzucco L, Burlando B. 2008. Platelet lysate stimulates wound repair of HaCaT keratinocytes. *Br J Dermatol* 159:537–545.
- Romagnani P, Annunziato F, Lasagni L, Lazzeri E, Beltrame C, Francalanci M, Uguccioni M, Galli G, Cosmi L, Maurenzi L, Baggiolini M, Maggi E, Romagnani S, Serio M. 2001. Cell cycle-dependent expression of CXC chemokine receptor 3 by endothelial cells mediates angiostatic activity. *J Clin Invest* 107:53–63.
- Ross R. 1993. The pathogenesis of atherosclerosis: A perspective for the 1990s. *Nature* 362:801–809.
- Sammak PJ, Hinman LE, Tran PO, Sjaastad MD, Machen TE. 1997. How do injured cells communicate with the surviving cell monolayer? *J Cell Sci* 110:465–475.
- Schmitt JM, Wayman GA, Nozaki N, Soderling TR., 2004. Calcium activation of ERK mediated by calmodulin kinase I. *J Biol Chem*. 279:24064–24072.
- Shiojima I, Walsh K. 2002. Role of Akt signaling in vascular homeostasis and angiogenesis. *Circ Res* 90:1243–1250.

Soffer E, Ouhayoun JP, Anagnostou F. 2003. Fibrin sealants and platelet preparations in bone and periodontal healing. *Oral Surg Oral Med Oral Pathol Oral Radiol Endod* 95:521–528.

Whang K, Goldstick TK, Healy KE. 2000. A biodegradable polymer scaffold for delivery of osteotropic factors. *Biomaterials* 21:2545–2551.

Xiao YQ, Malcolm K, Worthen GS, Gardai S, Schiemann WP, Fadok VA, Bratton DL, Henson PM., 2002. Cross-talk between ERK and p38 MAPK mediates selective suppression of pro-inflammatory cytokines by transforming growth factor-beta. *J Biol Chem*. 277:14884–14893.

Xu KP, Riggs A, Ding Y, Yu FS. 2004. Role of ErbB2 in corneal epithelial wound healing. *Invest Ophthalmol Vis Sci* 45:4277–4283.